Available online at www.sciencedirect.com
SCIENCE DIRECT®
Journal of Luminescence 104 (2003) 47–54
JOURNAL OF LUMINESCENCE
www.elsevier.com/locate/jlumin

Improving the efficiency of a blue-emitting phosphor by an energy transfer from Gd^{3+} to Ce^{3+}

E.J. Bosze[a], G.A. Hirata[a,b], L.E. Shea-Rohwer[c], J. McKittrick[a,*]

[a] *Department of Mechanical and Aerospace Engineering and Materials Science and Engineering Program, University of California, San Diego, 9500 Gilman Drive, La Jolla, CA 92093-0411, USA*

[b] *Centro de Ciencias de la Materia Condensada, Universidad Nacional Autónoma de México, CP 22860, Ensenada, Baja California, Mexico*

[c] *Sandia National Laboratory, Albuquerque, NM 87185-0527, USA*

Received 6 June 2002; received in revised form 11 November 2002; accepted 11 November 2002

Abstract

The low-voltage efficiency of the blue-emitting phosphor, cerium activated yttrium silicate $(Y_{1-m}Ce_m)_2SiO_5$, has been improved by co-activating with gadolinium, $(Y_{1-m-n}Ce_mGd_n)_2SiO_5$. Gd^{3+} improves the efficiency by transferring energy to Ce^{3+}, and makes this phosphor a more promising candidate for low-voltage field emission flat panel displays. Low-voltage cathodoluminescence and photoluminescence measurements were made to determine the optimum concentrations of Gd^{3+} that yielded the most luminous efficient phosphor. For photoluminescence, Ce^{3+} most efficiently luminesces at the excitation wavelength $\lambda_{ex} = 358$ nm. Co-activating with Gd^{3+} did not improve the photoluminescent efficiency because Gd^{3+} does not absorb at Ce^{3+} excitation energy, and thus cannot transfer energy. For low-voltage cathodoluminescence, co-activating with Gd^{3+} did improve the efficiency since Gd^{3+} was sufficiently excited, with the optimum composition found to be $(Y_{0.8425}Ce_{0.0075}Gd_{0.15})_2SiO_5$.

PACS: 78.55.−m; 78.60.−b

Keywords: Cathodoluminescence; Photoluminescence; Luminescence efficiency; Energy transfer

1. Introduction

Field emission displays (FED) are the next generation flat panel display design that utilizes cathodoluminescence (CL) to excite phosphors, similar to the mature cathode-ray tubes (CRTs). CRTs are large, but offer a bright screen and good contrast due to the high amount of energy, between 15 and 30 keV, the electrons impart onto the phosphor-coated screen. In FED technology, the electron gun is replaced by a matrix-addressed array of hundreds of millions of ~1 μm inverted conical electron field emitter tips deposited onto a flat substrate. The distance between the emitter tips and the phosphor coated screen is greatly reduced from that distance between the electron gun and the screen in CRTs (0.1 cm compared with ~45 cm). Thus, the acceleration voltages are

*Corresponding author. Tel.: +1-619-534-5425; fax: +1-619-534-5698.

E-mail address: jmckittrick@ucsd.edu (J. McKittrick).

0022-2313/02/$ - see front matter © 2002 Elsevier Science B.V. All rights reserved.
doi:10.1016/S0022-2313(02)00663-4

reduced to as low as possible in order to prevent damaging coronal discharge between the electron emitters and the screen [1]. While lower voltages decrease the power consumption of the FED from that of the CRT, the lower energy electrons reduce the brightness and color gamut of the screen. To keep the brightness and color gamut competitive with that of CRTs, the current density is increased. This leads to higher coulombic loading, or aging, which accelerates the chemical disassociation and causes defects that decrease the efficiency of the phosphors [1]. When sulfur containing phosphors are used in the FED environment, the dissociated sulfur ions can damage the electron emitter tips by raising their work function and cause the eventual failure of the FED screen. Age-resistant coatings that encase the phosphor particles are currently being developed [2]. When an electron hits the age-resistant coating, most of its energy is absorbed by the coating, reducing the energy imparted on the phosphor and leading to reduced emission [1]. Therefore, phosphors must be developed that exhibit efficient luminescence with good chromaticity coordinates, and also withstand the high coulombic loading from the field emitter tips. Oxide host lattice phosphors show the most promise in meeting these requirements.

Cerium (Ce^{3+}) activated yttrium silicate, $(Y_{1-m}Ce_m)_2SiO_5$, is currently being used[1] as the blue component phosphor for low-voltage flat panel FEDs. Yttrium silicate is isostructural with the monoclinic rare-earth (RE) oxyorthosilicates, $RE_2(SiO_4)O$, which crystallize into two different structures, denoted X_1 and X_2 [3,4]. X_1 crystallizes for the large RE ions lanthanum to terbium (radii of 0.092–0.114 nm) with the space group $P2_1/c$. The RE ions occupy two crystallographic sites that exhibit C_1 symmetry, denoted A1 and A2. Site A1 has a coordination number (CN) of 9, with 8 oxygens bonded to silicon and one free oxygen. Site A2 has a CN of 7, with 4 oxygens bonded to silicon and 3 free oxygens. X_2 crystallizes for the smaller RE ions dysprosium to lutetium (radii of 0.085–0.092 nm), with the space group C2/c. The RE ions also occupy two different crystallographic sites with C_1 symmetry, denoted B1 and B2. B1 has a CN of 6 and site B2 has a CN of 7, with both sites having two free oxygens [5]. To form Y_2SiO_5, yttrium (Y^{3+}) replaces the RE ion in these structures (radius of 0.093 nm) and forms either the X_1 or X_2 polymorphs depending on the preparation. X_1, the low-temperature polymorph, forms at temperatures less than 1190°C while X_2, the high-temperature polymorph, forms at temperatures above 1190°C [6], and has a melting temperature of 1980°C [7].

The activator Ce^{3+} (radius of 0.106 nm) can easily substitute for Y^{3+}, and equally populates the two different crystallographic sites in the X_1- and X_2-Y_2SiO_5 structures. Fig. 1(a) shows the photoluminescence (PL) emission spectra of $(Y_{1-m}Ce_m)_2SiO_5$ for the X_1- and X_2-Y_2SiO_5. X_2 is the desired phase due to its higher luminescent efficiency and more saturated blue-emission which leads to more favorable chromaticity values. The luminescence arises from the parity allowed f→d electronic transition in Ce^{3+}. Fig. 2(a) shows the energy level diagram for Ce^{3+} in Y_2SiO_5, in which luminescence occurs from the 5d to either the $^2F_{7/2}$ or $^2F_{5/2}$ ground state [8]. The split in the ground state level is due to the electrons exhibiting either a $+\frac{1}{2}$ or $-\frac{1}{2}$ spin which causes the doublet emission seen in both the X_1- and X_2-Y_2SiO_5 spectra. The

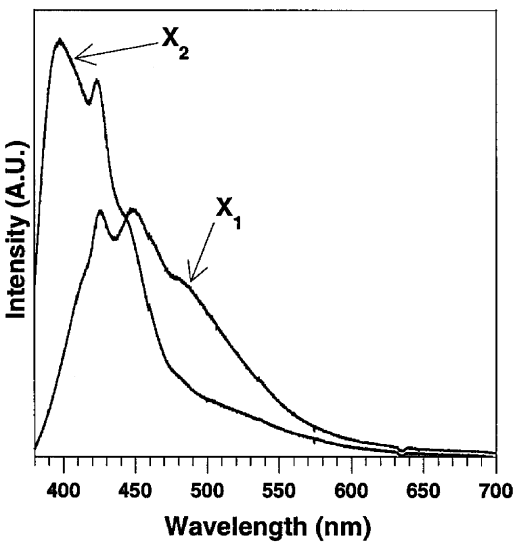

Fig. 1. Luminescence spectra from the low-temperature X_1-Y_2SiO_5 and high-temperature X_2-Y_2SiO_5 structures of $(Y_{1-m}Ce_m)_2SiO_5$ (same scale).

[1] Futaba Corp. of America, Schaumburg IL 60173, USA.

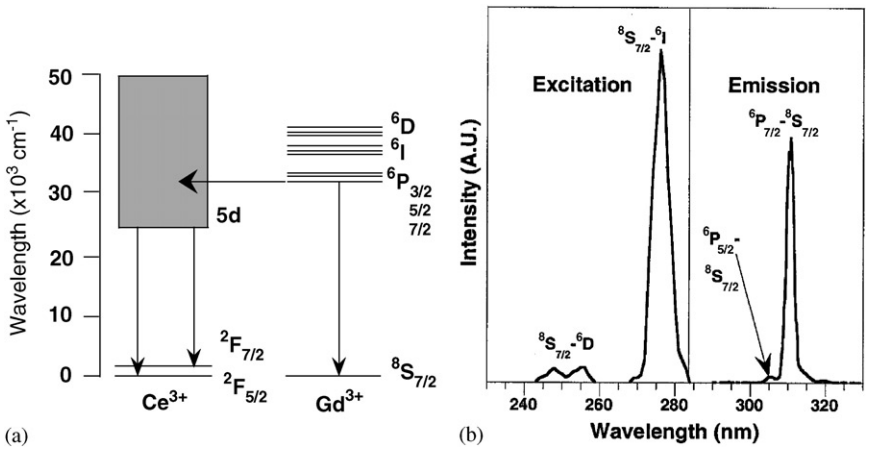

Fig. 2. (a) Energy level diagram of Ce^{3+} and Gd^{3+} in yttrium silicate. (b) Excitation and emission spectra of Gd^{3+} in yttrium silicate.

emission properties attributed to the A1 and A2 sites in the X_1-Y_2SiO_5 have been shown to be identical, as they have for the B1 and B2 sites in the X_2-Y_2SiO_5 [5]. The allowed electronic transition also gives rise to the broad asymmetric emission that stretches into the green and red regions of the visual spectrum. A possible explanation to describe the asymmetric emission could be offered by the Jahn–Teller effect. The emission from Ce^{3+} arises from a 5d state in which the energy levels are highly influenced by the surrounding O^{2-} ligands. Since not all bonds between the Ce^{3+} and O^{2-} ligands are of the same length, the emission from these states could cause the emission to become distorted towards the longer wavelengths. There is some evidence that the Jahn–Teller effect can influence the emission from Ce^{3+} in $Y_3Al_5O_{12}$ [9].

The luminescent efficiency can be improved by substituting Y^{3+} with Gd^{3+} (radius of 0.097 nm). Gd^{3+} can readily transfer energy to other rare-earth ions because the energy difference between its ground and first excited state is the largest for all trivalent rare-earth ions, greater than 30,000 cm^{-1} [10]. Fig. 2(a) shows the energy level diagram of Gd^{3+}, and (b) shows its excitation and emission spectra. In Y_2SiO_5, Gd^{3+} emission mainly occurs at 313 and 307 nm. The emission at 313 nm is due to the electric-dipole transition $^6P_{7/2} \rightarrow {}^8S_{7/2}$, while the emission at 307 nm is due to the magnetic-dipole transition $^6P_{5/2} \rightarrow {}^8S_{7/2}$. Due to the forbidden nature of the ^{6}I and ^{6}D transitions, only when Gd^{3+} is sufficiently excited via energy transfer from the host lattice can Gd^{3+} further transfer energy to Ce^{3+} [10]. Energy transfer occurs because the $^6P_{7/2}$ energy level of Gd^{3+} is equal to the 5d levels of Ce^{3+}, shown in Fig. 2(a), and is known as the resonance condition [11]. Resonance takes place because the emission of Gd^{3+} overlaps with the 310 nm absorption peak of Ce^{3+}. It has been previously shown that in single crystals of Ce^{3+} activated yttrium silicate, Gd^{3+} improved the cathodoluminescence efficiency by 50%, with an optimal composition found to be $(Y_{0.9725}Ce_{0.0025}Gd_{0.025})_2SiO_5$ [12].

The purpose of this study is to improve the low-voltage cathodoluminescence efficiency of $(Y_{1-m}Ce_m)_2SiO_5$ by co-activating with Gd^{3+}, $(Y_{1-m-n}Ce_mGd_n)_2SiO_5$, and determining the optimum composition that achieves the maximum luminous output at low-voltage excitation. Phosphor powders with various activator and co-activator concentrations were measured using photoluminescence and cathodoluminescence (500–5000 eV) to determine the optimum composition.

2. Experimental

Yttrium silicate, $(Y_{1-m-n}Ce_mGd_n)_2SiO_5$, phosphors were prepared using combustion synthesis. Combustion synthesis involves a highly

exothermic reaction between metal nitrates and an organic fuel, producing temperatures in excess of 1500°C, and sustains these high temperatures long enough (~45 s for a complete reaction) for the product to crystallize and grow. The reactant materials were $Y(NO_3)_3 \cdot 6H_2O$ (Alfa Æsear REacton 99.99% [REO]), $Ce(NO_3)_3 \cdot 5H_2O$ (Alfa Æsear REacton 99.99% [REO]), $Gd(NO_3)_3 \cdot 6H_2O$ O (Alfa Æsear REacton 99.99% [REO]), fumed 0.014 μm SiO_2 (Aldrich 99.9%) and carbohydrazide (CH_6N_4O) (Aldrich 98%). The reactants were weighed to make several compositions according to the reaction,

$$\begin{aligned} &2(1-m-n)Y(NO_3)_3 + 2mCe(NO_3)_3 \\ &\quad + 2nGd(NO_3)_3 + SiO_2 + \tfrac{15}{4}CH_6N_4O \\ &= (Y_{1-m-n}Ce_mGd_n)_2SiO_5 + \tfrac{15}{4}CO_2 \\ &\quad + \tfrac{45}{4}H_2O + \tfrac{21}{2}N_2, \end{aligned} \tag{1}$$

where m ranged from 0.001 to 0.05 and n ranged from 0.05 to 0.30. The precursors were placed into a 300 ml pyrex crystallization dish and dissolved in 50 ml of water. The solution was stirred for 30 min with a magnetic stirring bar and put into a preheated muffle furnace at 500°C. Once the water boiled, the reactants ignited, producing a porous powder that filled the volume of the crystallization dish. The porosity is caused by evolved gases, with the reaction forming 25 mol of gas for every 1 mole of solid Y_2SiO_5 formed. More information on combustion synthesis can be found elsewhere [13–15]. The product was allowed to cool and then lightly grounded for a few minutes with an alumina mortar and pestle. A fraction of each composition was then annealed at 1350°C for 1 h to fully transform the powders to the desired X_2-Y_2SiO_5 phase. The phases present were determined by X-ray diffraction (XRD), using $CuK_{\alpha 1}$ (0.15406 nm) radiation. Particle size and morphology were determined using a scanning electron microscope (SEM). The photoluminescent (PL) properties and low-voltage cathodoluminescent (CL) efficiencies (lm/W) were determined for annealed powders and compared to commercial standards from Nichia[2] and USR Optonix[3] which appeared to be prepared via a solid state synthesis reaction. The emission spectra and luminescent intensity for PL were measured using a 450 W xenon lamp, excitation and emission monochromators (both with 1200 groves/mm gratings) and a 1024 × 124 CCD camera to record the emission spectra. The CL efficiencies were measured in the projected voltage range of FEDs, 500–5000 eV, using a spot size of 0.196 cm^2 at a constant 5 mW/cm^2 power. The emitted light was coupled into an optical fiber bundle leading to a spectroradiometer. The light was dispersed by a 400 groves/mm grating and imaged with a 1024 element linear silicon photodiode array. The resulting spectrum was then weighted by the photonic response of the eye and integrated over the range of visible wavelengths. The result of this calculation was the luminous intensity per unit area in candelas per meter square (cd/m^2). The efficiency was then calculated by

$$\varepsilon = \frac{\text{lm}}{\text{W}} = \frac{\pi \times \text{luminance(cd/m}^2) \times \text{spotsize(m}^2)}{\text{volts} \times \text{amps}}. \tag{2}$$

3. Results and discussion

Fig. 3 shows the XRD patterns for combustion synthesized yttrium silicate powders, both as-synthesized and annealed at 1350°C for 1 h, with a commercial standard shown as a reference. The only identifiable phases present in the as-synthesized powders were the X_1- (marked with an *, JCPDS Card # 41-4 [16]) and X_2-Y_2SiO_5 (JCPDS Card #37-1476 [16]) polymorphs, with no unreacted SiO_2 or Y_2O_3 found. X_2-Y_2SiO_5 was the major phase found in the annealed and commercial powders. The annealed combustion synthesized powder has an unidentified peak at $2\theta = 29.2°$. The peak closely corresponds to the 80% peak of X_1-Y_2SiO_5 (29.24°) and to the 100% peak of Y_2O_3 ($2\theta = 29.15°$) (JCPDS Card 41-1105). No other unindexed peaks were detected.

PL and CL emission spectra for $(Y_{1-m}Ce_m)_2SiO_5$ were found to be similar. The optimum Ce^{3+} concentration was found

[2] 3775 Hempland Road, Mountville, PA 17554.
[3] 214 Kings Highway, Hackettstown, NJ 07840.

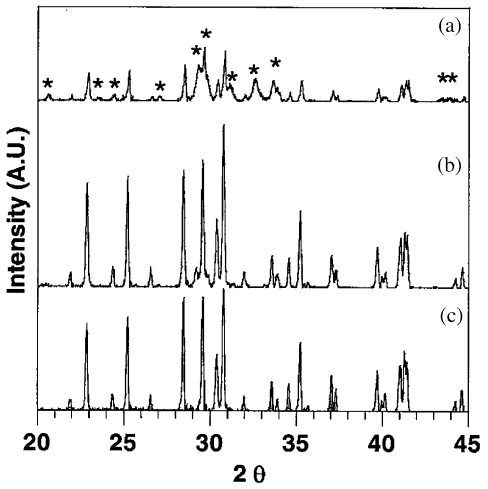

Fig. 3. XRD scans of (a) as-synthesized powders (* denotes X_1-Y_2SiO_5) and (b) after being annealed at 1350°C for 1 h and are compared to (c) a Y_2SiO_5:Ce commercial standard.

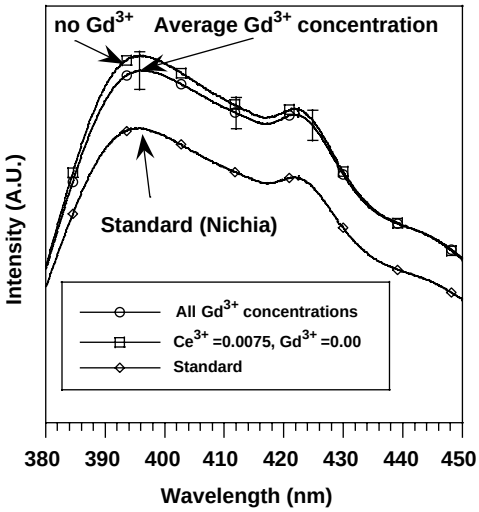

Fig. 4. The PL spectra for powders with a composition $(Y_{0.9925-n}Ce_{0.0075}Gd_n)_2SiO_5$ and is compared to $(Y_{0.9925}Ce_{0.0075})_2SiO_5$ and a commercial standard. Error bars are associated with spectra containing various Gd^{3+} concentrations ($\lambda_{ex} = 358$ nm).

previously, with $m = 0.0075$ for both PL and low-voltage CL ($\leqslant 1$ keV) [17]. From PL absorption spectra, the maximum excitation wavelength was found to be 358 nm, with smaller absorption lines occurring around 310, 275 and 220 nm and an adsorption edge at approximately 200 nm [17]. These results agree for $(Y_{0.99}Ce_{0.01})_2SiO_5$ powders made via sol–gel synthesis [5].

$(Y_{0.9925-n}Ce_{0.0075}Gd_n)_2SiO_5$ was co-activated with Gd^{3+} with concentrations ranging from $n = 0.05$ to 0.30. Under PL excitation, emission only occurs when exciting at Ce^{3+} maximum excitation wavelength, $\lambda_{ex} = 358$ nm, or exciting the host lattice which occurs at wavelengths less than 220 nm. When exciting at Gd^{3+} excitation wavelengths, 273 nm ($^8S_{7/2} \rightarrow {}^6I$) and around 250 nm ($^8S_{7/2} \rightarrow {}^6D$), the luminescence is much less than at Ce^{3+} excitation wavelength due to the absorption of these wavelengths being weak for both Ce^{3+} and Gd^{3+}. Fig. 4 shows the emission at $\lambda_{ex} = 358$ nm for a powder containing no Gd^{3+} and the average emission for all powders containing Gd^{3+}, and demonstrates that Gd^{3+} does not improve the luminescent intensity when excited at this wavelength. Therefore, exciting this phosphor at wavelengths longer than approximately 220 nm does not provide enough energy to excite Gd^{3+} and for energy transfer to occur.

While the addition of Gd^{3+} did not improve the PL intensity, it was found to improve the CL efficiency. Fig. 5(a) shows how the composition (Ce^{3+} concentration held constant at $m = 0.0075$, Gd^{3+} ranging from $n = 0.05$–0.30) affected the efficiency and is compared to a commercial standard. Fig. 5(b) shows the efficiency normalized to a commercial standard (standard = 1.0), at each voltage, in Fig. 5(a). The optimal composition, shown in Fig. 5, is $(Y_{0.8425}Ce_{0.0075}Gd_{0.15})_2SiO_5$ and was found to have improved efficiencies of 5–60% over the commercial standards at voltages lower than approximately 2 keV. At excitation voltages higher than 2 keV, the efficiencies of commercial phosphors were found to be comparable to the optimally activated combustion synthesized phosphor. In addition, no emission from Gd^{3+} was detected in the emission spectra from the commercial standards. The Ce^{3+} and Gd^{3+} concentrations are also much higher than those reported for single crystals in Ref. [12]. Powders have numerous lattice defects which quench the emission intensity. In single crystals, lattice defects are at a minimum, but energy transfer between like activators that promote concentration quenching

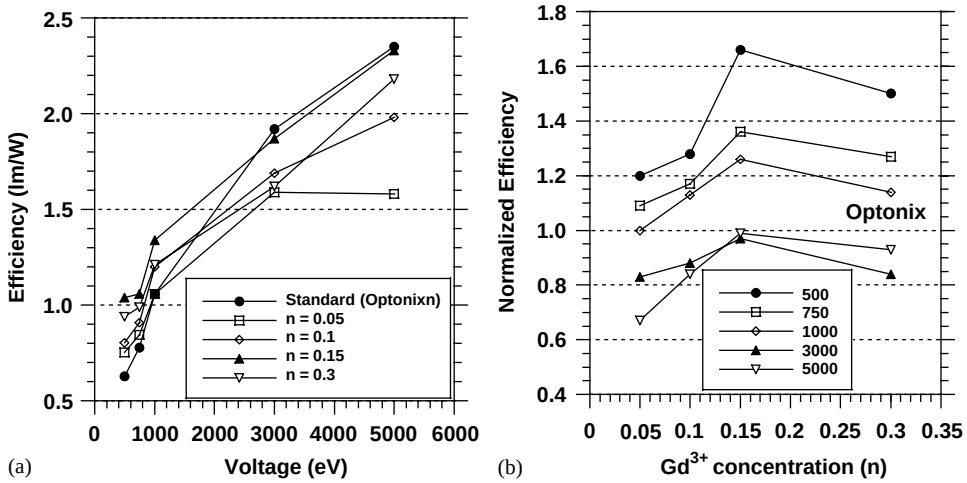

Fig. 5. (a) CL efficiency as a function of voltage for $(Y_{0.9925-n}Ce_{0.0075}Gd_n)_2SiO_5$. (b) CL efficiency normalized to a standard as a function of the Gd^{3+} concentration.

increase, which decreases the emission intensity once the activator concentration is higher than some optimal level. Therefore, lower activator concentrations are needed to keep this energy transfer at a minimum. In powders, higher activator concentrations increase the number of activators in crystallographic sites that prompt luminescence, but defects decrease the interaction between activators since they are also competing to absorb the incident energy. Defects absorb the incident energy, which decreases the amount of energy reaching the activator ions, which decrease the luminescence.

Fig. 6 shows the emission spectra of powders containing Gd^{3+} compared with a commercial standard. As the Gd^{3+} concentration increases from $n = 0.05$ to 0.30, the emission intensity of Gd^{3+} decreases, while the emission from Ce^{3+} increases until the Gd^{3+} concentration reaches 0.15. As the concentration of Gd^{3+} increases above $n = 0.15$, concentration quenching reduces the emission of Gd^{3+} further. Eventually, at higher concentrations, Gd^{3+} will no longer emit and the crystalline structure will revert to X_1 when Gd^{3+} fully replaces Y^{3+}, forming Gd_2SiO_5. The Ce^{3+} emission in Gd_2SiO_5 is similar to that of X_1-Y_2SiO_5:Ce.

There are several explanations for the better performance of the optimally activated combustion synthesized phosphor over the commercial standards at voltages $\leqslant 2$ keV. One explanation is that the composition of the commercial powders is optimized for higher voltage applications. Secondly, at low voltages, the electrons do not penetrate deeply into the phosphor particle, leaving a large number of activators unexcited. Since Gd^{3+} readily transfers energy to Ce^{3+}, the optical activity of Ce^{3+} is increased as is the

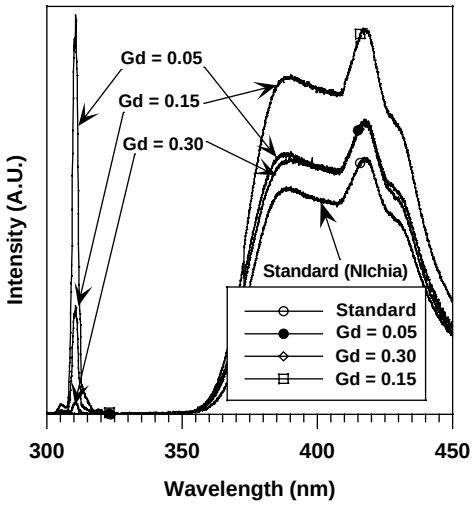

Fig. 6. The effect of Gd^{3+} concentration on the CL luminescent spectra (1 keV excitation).

number of excited Ce^{3+}, which yields higher efficiencies at low voltages. At higher excitation voltages, most Ce^{3+} and Gd^{3+} ions are excited due to deeper penetration of electrons into the particles. Since there is only a limited number of activators which are excited both by the electron beam and from energy transfer from Gd^{3+}, the phosphor may have reached saturation. By adding higher concentrations of Ce^{3+}, the efficiency could be improved beyond that seen with the commercial standards. Once the Ce^{3+} concentration exceeds an optimal level, concentration quenching between Ce^{3+} ions would decrease the emission intensity and the addition of Gd^{3+} would not improve the efficiency.

The chromaticity of the optimally activated combustion synthesized powders under CL excitation was found to be comparable to the commercial standards at low excitation voltages. The average chromaticity values were $x = 0.159$ and $y = 0.109$ for the optimally activated phosphor and $x = 0.161$ and $y = 0.126$ for the commercial standards. The chromaticity values were not found to vary significantly over the range of excitation voltages used or with Gd^{3+} concentration. These values are also better than the chromaticity values for X_1-Y_2SiO_5:Ce, $x = 0.181$ and $y = 0.198$. The optimum chromaticity values are from the blue CRT phosphor ZnS:Ag, $x = 0.147$ and $y = 0.054$. Fig. 7 plots the chromaticity coordinates for the X_1- and X_2-Y_2SiO_5 phosphors and the blue CRT phosphor. The emission spectra of X_2-Y_2SiO_5 would also exhibit a saturated blue if it was not for the long emission tail that extends into the green and red regions of the visual spectra. The emissions from the tail mix with the saturated blue doublet emission from the main transitions in Ce^{3+}, and give the phosphor a blue-white hue, which would slightly reduce the color gamut of a display screen.

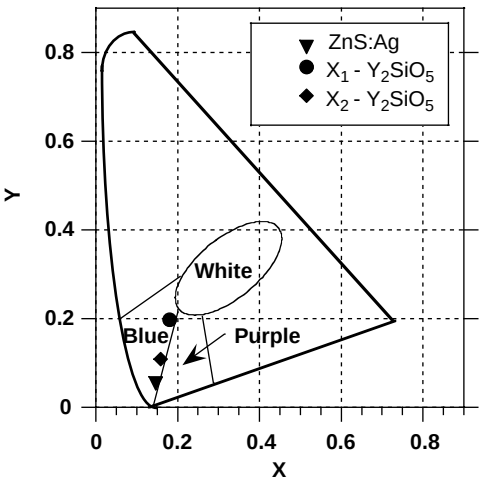

Fig. 7. Chromaticity coordinates of X_1- and X_2-$(Y_{1-m}Ce_mGd_n)_2SiO_5$ compared to the $(Zn_{1-x}Ag_x)S$ blue CRT phosphor.

4. Conclusions

The low-voltage cathodoluminescence efficiency of cerium activated yttrium silicate has been improved by co-activating with Gd^{3+}, $(Y_{1-m-n}Ce_mGd_n)_2SiO_5$. The low-voltage cathodoluminescence efficiency was enhanced via energy transfer from Gd^{3+} to Ce^{3+}. The optimum Gd^{3+} concentration was found to be $n = 0.15$, with the optimum phosphor composition found to be $(Y_{0.8425}Ce_{0.0075}Gd_{0.15})_2SiO_5$. The optimum concentrations of Ce^{3+} and Gd^{3+} are higher than for single crystals due to the defects in the powder competing with these activators with absorbing and re-emitting the incident energy. The optimally activated powdered phosphor was found to be better than commercial standards up to voltages of around 2 kV, while at higher voltages it was found to be only slightly less efficient. While this phosphor has an efficiency of approximately 1 lm/W at 1 kV which is required for a good blue-emitting candidate for low-voltage field emission flat panel displays, its chromaticity coordinates were found to be less optimal than the blue-emitting CRT phosphor.

Acknowledgements

The authors would like to acknowledge the financial support of the Phosphor Technology Center of Excellence by DARPA Grant No. MDA972-92-1-0030 and the National Science Foundation, Grant No. DMR9972509.

References

[1] P.H. Holloway, J. Sebastian, T. Trottier, S. Jones, H. Swart, R.O. Peterson, in: M.K. Hatalis, J. Kanicki, C.J. Summers, F. Funada (Eds.), Flat Panel Display Materials II, Materials Research Society Proceedings, Vol. 424, Materials Research Society, San Francisco, CA, 1997, pp. 425–431.
[2] Y. Fran, T. Tseng, Mater. Chem. Phys. 61 (1999) 166–168.
[3] M. Leskelä, J. Suikkanen, J. Less-Common Metals 112 (1985) 71–74.
[4] J. Reichardt, M. Stiebler, R. Hirrle, S. Kemmler-Sack, Phys. Stat. Sol. A 119 (1990) 631–642.
[5] J. Lin, Q. Su, H. Zhang, S. Wang, Mater. Res. Bull. 31 (1996) 189–196.
[6] J. Wang, S. Tian, G. Li, F. Liao, X. Jing, Mater. Res. Bull. 36 (2001) 1855–1861.
[7] E.M. Levin, C.R. Robbins, H.F. McMurdie, Phase Diagrams for Ceramists, Vol. 2, American Ceramic Society, Columbus, 1964, p. 2388.
[8] T. Kano, Principal phosphor materials and their optical properties, in: W.M. Yen (Ed.), Phosphor Handbook, CRC Press, New York, 1999, pp. 177–200.
[9] M. Grinberg, A. Sikorska, S. Kaczmarek, J. Alloys Compounds 300–301 (2000) 158–164.
[10] G. Blasse, Chemistry and physics of R-activated phosphors, in: L.R. Eyring (Ed.), Handbook on the Physics and Chemistry of Rare Earths, North-Holland Publishing Company, Amsterdam, 1979, pp. 237–274.
[11] G. Blasse, B.C. Grabmaier, Luminescent Materials, Springer, Berlin, 1994.
[12] J. Shmulovich, G.W. Berkstresser, C.D. Brandle, A. Valentino, J. Electrochem. Soc. 135 (1988) 3141–3151.
[13] L.E. Shea, J. McKittrick, O.A. Lopez, J. Amer. Ceram. Soc. 79 (1996) 3257–3265.
[14] J. McKittrick, L.E. Shea, C.F. Bacalski, E.J. Bosze, Displays 19 (1999) 169–172.
[15] J.J. Kingsley, K.C. Patil, Mater. Lett. 6 (1988) 427–432.
[16] JCPDS, Joint Committee on Powder Diffraction Standards: International Centre for Diffraction Data (ICDD), 12 Campus Blvd., Newtown Square, PA 19073.
[17] E.J. Bosze, G.A. Hirata, J. McKittrick, L.E. Shea, in: G.N. Parsons, C.-C. Tsai, T.S. Fahlen, C.H. Seager (Eds.), Flat-Panel Display Materials, Materials Research Society Proceedings, Vol. 508, Materials Research Society, San Francisco, CA, 1998, pp. 269–274.